

## Nearly Perfect Triplet-Triplet Energy Transfer from Wannier Excitons to Naphthalene in Organic-Inorganic Hybrid Quantum-Well Materials

K. Ema, M. Inomata, Y. Kato, and H. Kunugita

*Department of Physics, Sophia University, 7-1 Kioi-cho, Chiyoda-ku, Tokyo 102-8554, Japan*

M. Era

*Department of Chemistry and Applied Chemistry, Saga University, 1 Honjo-machi, Saga City, Saga 840-8502, Japan*

(Received 9 February 2008; published 25 June 2008)

We report the observation of extremely efficient energy transfer (greater than 99%) in an organic-inorganic hybrid quantum-well structure consisting of perovskite-type lead bromide well layers and naphthalene-linked ammonium barrier layers. Time-resolved photoluminescence measurements confirm that the transfer is triplet-triplet Dexter-type energy transfer from Wannier excitons in the inorganic well to the triplet state of naphthalene molecules in the organic barrier. Using measurements in the 10–300 K temperature range, we also investigated the temperature dependence of the energy transfer.

DOI: [10.1103/PhysRevLett.100.257401](https://doi.org/10.1103/PhysRevLett.100.257401)

PACS numbers: 78.67.De, 71.35.Gg, 73.21.Fg, 81.07.Pr

Organic-inorganic hybrid materials have attracted great interest because of their potential application to new types of optoelectronic devices [1–9]. In a typical hybrid material, low-dimensional Wannier excitons are formed in the inorganic part, and molecular excitations or Frenkel excitons are formed in the organic part. The most interesting property of such systems is their ability to couple these two different types of excitons. It has been shown theoretically that such coupled excitons (the so-called “hybrid excitons”) have unique optical features derived from both the large oscillator strength of the Frenkel excitons and the large nonlinearity of the Wannier excitons [1–4]. However, clear experimental observation of these unique features has not been reported yet. The essential preliminary step towards achieving the hybrid exciton is the realization of an efficient energy transfer between the inorganic and organic parts. There are few reports of energy transfer from inorganic Wannier excitons to organic excitation. Era *et al.* observed strongly enhanced phosphorescence from naphthalene molecules in organic-inorganic hybrid quantum-well (QW) materials and suggested that this is caused by an efficient energy transfer from excitons to the naphthalene molecules [10]. However, the mechanism of the efficient energy transfer was not clarified by them, because the fine structure of the exciton states in the inorganic layers was not clear at that time. Recently Blumstengel *et al.* and Itskos *et al.* reported Förster-type energy transfer [11] from Wannier excitons in inorganic QWs to organic layers [8,9]. They demonstrated efficient dipole-dipole energy transfer ( $\sim 50\%$ ) between Wannier and Frenkel excitons in hybrid material. There is another type of energy transfer mechanism other than the Förster type: the direct electron exchange (Dexter type) energy transfer [12]. For organic-inorganic hybrid materials there is no report on the Dexter-type energy transfer, although the Dexter mechanism is quite important for nanoscale interaction in hybrid materials [13].

In this Letter we report the direct observation of almost perfect energy transfer (over 99%) in naphthalene-incorporated layered perovskite-type quantum-well materials ( $\text{N-CnPbBr}_4$ ). We have found that the photoexcited energy is transferred from Wannier excitons in inorganic quantum wells to naphthalene molecules in organic barrier layers. The observed energy transfer rate is extremely large, greater than  $10 \text{ ns}^{-1}$ . Thanks to the recent understanding of the exciton fine structure [14,15], we have been able to describe the energy transfer mechanism using time-resolved photoluminescence (PL) measurements. Our results show that the observed energy transfer is the triplet-triplet Dexter-type transfer, thus achieving the first observation in organic-inorganic hybrid materials.

The layered perovskite-type quantum-well family  $(\text{C}_n\text{H}_{2n+1}\text{NH}_3)_2\text{PbX}_4$  ( $X = \text{I}, \text{Br}, \text{Cl}$ ) forms organic-inorganic hybrid QW systems, where inorganic well layers are composed of a two-dimensional network of corner-sharing  $[\text{PbX}_6]^{4-}$  octahedra between organic barrier layers of alkylammonium chains [16,17]. The well layers form monolayers without well-width fluctuation and the interface between the well and the barrier is intrinsically flat. These unique features come from the fact that they are ideal self-organized materials in which there are no stress and lattice mismatch at the interface. The schematic of the crystal structure of  $(\text{C}_n\text{H}_{2n+1}\text{NH}_3)_2\text{PbBr}_4$  (hereafter denoted as  $\text{CnPbBr}_4$ ) is shown in Fig. 1(a). Owing to the quantum confinement and dielectric enhancement effects ( $\epsilon_{\text{well}} = 4.8$ ,  $\epsilon_{\text{barrier}} = 2.1$ ), the excitons are tightly confined in the inorganic well layers and form two-dimensional (2D) Wannier excitons [14,17,18].

Figure 1(b) shows the energy structure and decay dynamics of the excitons in  $\text{C4PbBr}_4$ .  $\Gamma_5^-$  excitons are dipole-allowed singlet excitons, while  $\Gamma_2^-$  and  $\Gamma_1^-$  excitons are mainly composed of triplet excitons [15]. In the present study, the spectral resolution was not high enough to resolve the  $\Gamma_2^-$  and  $\Gamma_1^-$  levels. Therefore, we call excitons

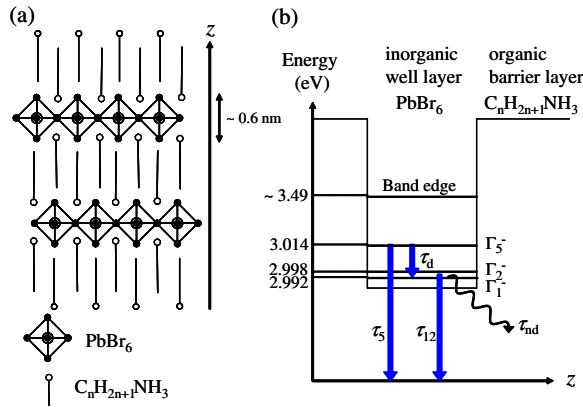


FIG. 1 (color online). (a) Schematic of the crystal structure of C4PbBr4. (b) Energy diagram and decay dynamics of the excitons in the inorganic well.

in these levels  $\Gamma_{1,2}^-$  excitons. Optical excitation above the band gap of the inorganic well layer creates the  $\Gamma_5^-$  and  $\Gamma_{1,2}^-$  excitons. However, the  $\Gamma_5^-$  excitons quickly relax to  $\Gamma_{1,2}^-$  excitons due to a spin relaxation of within several picoseconds, leaving relatively small populations at the  $\Gamma_5^-$  level. Since the  $\Gamma_{1,2}^-$  excitons have a relatively long lifetime (1–10 ns), many excitons are accumulated in the  $\Gamma_{1,2}^-$  levels. Therefore, the intensity of the singlet  $\Gamma_5^-$  emission is weaker than that of the  $\Gamma_{1,2}^-$  emissions in time-integrated PL measurements (see Fig. 3).

Figure 2(a) shows the schematic of the crystal structure of N-CnPbBr4 [10]. The basic structure is the same as that of C4PbBr4, except that the naphthalene molecules are linked to the alkyl chains. In this case, the energy structure, including the barrier layers, becomes the one shown in Fig. 2(b). The excited singlet state ( $S_1$ ) is located above the band edge of the well layer and the excited triplet state ( $T_1$ ) is located at and below the exciton levels. The  $S_1$  and  $T_1$  levels are widely distributed due to the molecular vibronic bands. When we excite the excitons in the well layer, we can expect the energy transfer from the accumulated  $\Gamma_{1,2}^-$  excitons to the naphthalene  $T_1$

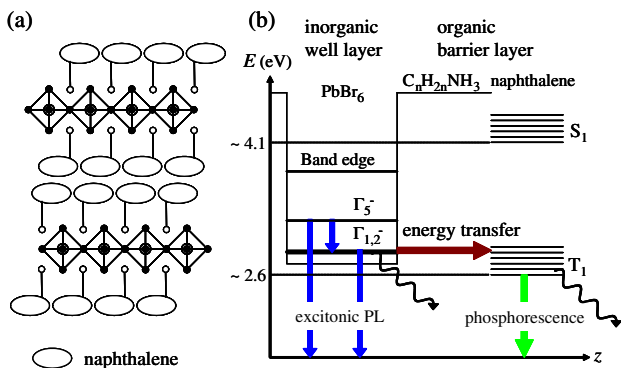


FIG. 2 (color online). (a) Schematic of the crystal structure of N-Cn. (b) Energy diagram and energy transfer dynamics of N-Cn.

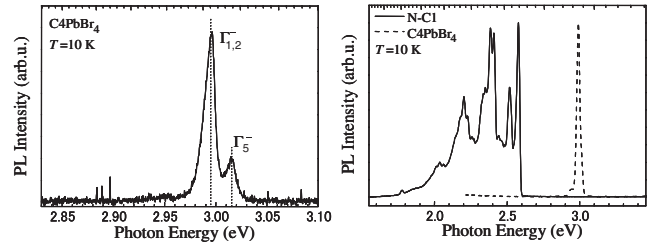


FIG. 3. PL spectra of C4PbBr4 and N-C1. For C4PbBr4, the excitonic PL (left graph and dashed line in right graph) is clearly observed, while N-C1 shows strongly enhanced phosphorescence (solid line in right graph) from the naphthalene molecules instead of the excitonic PL.

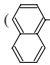
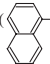
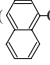
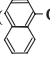
states. The back transfer from the naphthalene does not occur, because relaxation in the naphthalene vibronic band is quite fast (less than a picosecond).

For PL measurements the pulse duration and the repetition rate were 150 fs and 100 kHz, respectively. In order to investigate the mechanism of the energy transfer, the excitation energy was set to 3.54 eV, which is below the energy of the naphthalene singlet state but above the band edge of the well layer. The excitation power was weak enough to avoid biexcitonic influences. We used an optical multichannel analyzer for PL spectra measurements, and a streak camera for time-resolved measurements.

Table I shows the crystal structures of the samples. We controlled the length of the alkyl chains to change the distance between the naphthalene molecules and the inorganic well layer. This distance,  $R$ , was estimated from x-ray analysis.

Figure 3 shows the PL spectra of C4PbBr4 and N-C1 at 10 K. For C4PbBr4, the excitonic PL ( $\Gamma_5^-$  and  $\Gamma_{1,2}^-$  emissions) is clearly observed around 3.0 eV. On the other hand, N-C1 shows strongly enhanced phosphorescence from the triplet state of naphthalene molecules instead of the excitonic PL. The phosphorescence was extremely bright. This is in strong contrast to the fact that naphthalene derivatives do not usually exhibit phosphorescence. Although one of the reasons for the strong emission is the presence of the

TABLE I. Crystal structure of the samples.

| Name | Chemical formula   | $R$ (nm) |
|------|--|----------|
| N-C1 |  $(\text{C}_6\text{H}_4\text{CH}_2\text{NH}_3)_2\text{PbBr}_4$              | 0.11     |
| N-C2 |  $(\text{C}_6\text{H}_4\text{C}_2\text{H}_4\text{NH}_3)_2\text{PbBr}_4$     | 0.22     |
| N-C3 |  $(\text{C}_6\text{H}_4\text{OC}_3\text{H}_6\text{NH}_3)_2\text{PbBr}_4$    | 0.32     |
| N-C6 |  $(\text{C}_6\text{H}_4\text{OC}_6\text{H}_{13}\text{NH}_3)_2\text{PbBr}_4$ | 0.65     |

heavy metal lead, the high phosphorescence intensity is a direct result of the efficient energy transfer from the excitons to the naphthalene triplet states.

In order to confirm the energy transfer, we analyzed the temporal evolution of the excitonic PL intensities for all samples. As shown in Fig. 3, the excitonic PL from N-C1 does not appear in the time-integrated spectrum, because it is hidden by the strong phosphorescence with a relatively long decay time ( $\sim 4.3$  ms). In time-resolved measurements, however, the excitonic PL can be observed just after the excitation. Figure 4(a) shows the temporal evolutions of the excitonic PL for all samples. The  $\Gamma_5^-$  emissions for all samples (dashed lines in Fig. 4(a)) have relaxation times of about 10 ps with slight dispersions which are not systematically dependent on the sample. On the other hand, the  $\Gamma_{1,2}^-$  emissions (closed circles in Fig. 4) show clear exponential decays which are apparently dependent on the sample. The naphthalene-incorporated materials show faster decays compared to that of C4PbBr<sub>4</sub> ( $\sim 4$  ns), and the samples with the shorter alkyl chains show faster decay times. From these results, we can confirm that energy transfer occurs from the  $\Gamma_{1,2}^-$  excitons and the efficiency of the energy transfer increases with decreasing alkyl-chain length.

We can make a simple estimation of the energy transfer rate  $k_{ET}$  from the observed PL decay time  $\tau_{PL}$  as

$$k_{ET} = 1/\tau_{ET} = 1/\tau_{PL} - 1/\tau_{12}, \quad (1)$$

where  $\tau_{ET}$  is energy transfer time, and  $\tau_{12}$  is the PL decay time of the  $\Gamma_{1,2}^-$  emissions for C4PbBr<sub>4</sub>, which is composed of radiative and nonradiative decay. From the estimated  $\tau_{ET}$ , we can calculate the efficiency of energy transfer  $\eta_{ET}$  as

$$\eta_{ET} = \tau_{12}/(\tau_{ET} + \tau_{12}). \quad (2)$$

Figure 4(b) shows  $k_{ET}$  and  $\eta_{ET}$  as a function of  $R$ . The observed values of  $\tau_{12}$  range from 1 ns to 10 ns depending

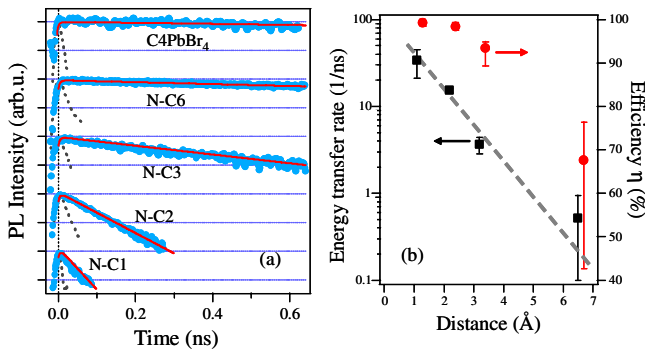


FIG. 4 (color online). (a) Time-resolved PL intensities for all samples at 10 K.  $\Gamma_{1,2}^-$  and  $\Gamma_5^-$  emissions are plotted by closed blue circles and dashed black lines, respectively. The solid red lines show calculated decay curves using Eqs. (3). (b) Dependence of the energy transfer rate (black squares) and the efficiency (red circles) on the distance between the exciton and the naphthalene. The dashed dark line is a guide to the eye.

on the sample quality. This variation of  $\tau_{12}$ , as well as the fitting variation of  $\tau_{PL}$ , is represented by the error bar. The estimated  $\eta_{ET}$  of N-C1 is greater than 99% ( $99.3^{+0.15}_{-0.8}\%$ ), which shows nearly perfect energy transfer. We can see that  $k_{ET}$  is almost exponentially dependent on  $R$ . This indicates that the energy transfer mechanism is Dexter type, since the Dexter transfer needs the overlap of exciton and naphthalene wave functions, and such overlap decreases exponentially with distance.

In the above simple analysis, we neglect the exciton dynamics in the inorganic well layers. In order to investigate the energy transfer in detail, we analyzed the temporal evolution of PL intensity with rate equations including the exciton dynamics;

$$\frac{dN_5}{dt} = -\left(\frac{1}{\tau_5} + \frac{1}{\tau_d}\right)N_5 + \frac{N_{12}}{\tau_u} + G(t), \quad (3a)$$

$$\frac{dN_{12}}{dt} = -\left(\frac{1}{\tau_{12}} + \frac{1}{\tau_u} + \frac{1}{\tau_{ET}}\right)N_{12} + \frac{N_5}{\tau_d} + G(t), \quad (3b)$$

where  $N_5$  ( $N_{12}$ ) is the population of the  $\Gamma_5^-$  ( $\Gamma_{1,2}^-$ ) exciton, and  $\tau_5$  ( $\tau_{12}$ ) is the lifetime of the  $\Gamma_5^-$  ( $\Gamma_{1,2}^-$ ) exciton. The generation rate of the excitons,  $G(t)$ , which is determined by the excitation pulse envelope at  $t = 0$ , is assumed to be the same for  $N_5$  and  $N_{12}$ .  $\tau_d$  and  $\tau_u$  are the transfer times from the  $\Gamma_5^-$  to the  $\Gamma_{1,2}^-$  levels and from the  $\Gamma_{1,2}^-$  to the  $\Gamma_5^-$  level, respectively. We assume that the ratio  $\tau_d/\tau_u$  is expressed using temperature  $T$  and the energy difference  $\Delta$  between the  $\Gamma_5^-$  (3.014 eV) and  $\Gamma_{1,2}^-$  (2.995 eV) levels;

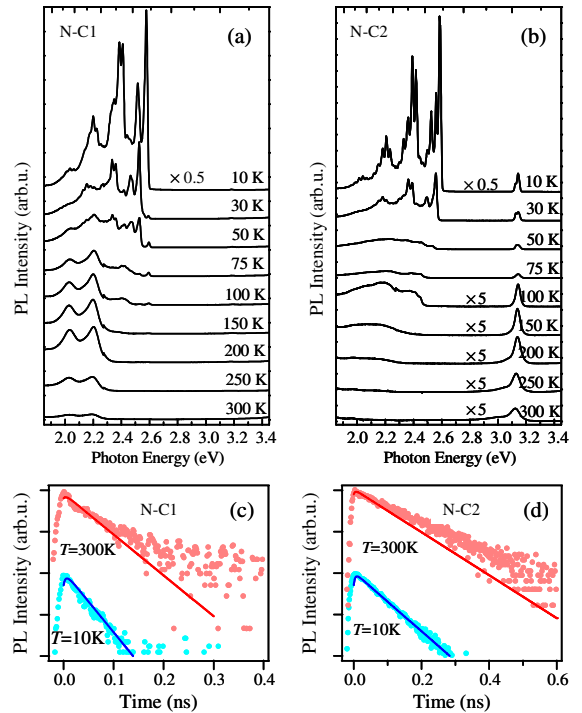


FIG. 5 (color online). Temperature dependence of PL spectra for N-C1 (a) and N-C2 (b). Calculated (solid lines) and observed (closed circles) PL decay curves for N-C1 (c) and N-C2 (d) at 10 and 300 K.

$$\frac{\tau_d}{\tau_u} = \frac{1 + \exp(-\Delta/k_B T)}{1 + \exp(\Delta/k_B T)}. \quad (4)$$

Using Eqs. (3) we can calculate the temporal change in the PL intensity of the  $\Gamma_{1,2}^-$  emissions. The values of the parameters we used in the calculation are  $\tau_5 = 300$  ps,  $\tau_{12} = 4$  ns,  $\tau_d(10 \text{ K}) = 4$  ps and  $\Delta = 20$  meV, as estimated from the data of C4PbBr<sub>4</sub>. The solid lines in Fig. 4(a) show the result of the calculation at  $T = 10$  K. Because  $1/\tau_u$  is negligible at 10 K, the calculated curves show the exponential decay and reproduce the experimental data. For higher temperatures the effect of  $\tau_u$  is no longer negligible; i.e., the conversion from  $\Gamma_{1,2}^-$  excitons to  $\Gamma_5^-$  excitons becomes significant. In this case, some parts of the population in the  $\Gamma_{1,2}^-$  levels go back to the  $\Gamma_5^-$  level instead of transferring to the naphthalene triplet states. Since the  $\Gamma_5^-$  excitons are dipole allowed, it can be anticipated that this  $\Gamma_{1,2}^-$  to  $\Gamma_5^-$  cycle makes the  $\Gamma_5^-$  emissions larger, and, consequently, the effective rate of energy transfer smaller.

Figures 5(a) and 5(b) show the temperature dependence of the PL spectra for N-C1 and N-C2. The total emission intensity decreases with increasing temperature because the nonradiative process becomes significant at high temperatures. When we focus on the intensity ratio of the phosphorescence to the excitonic emission in N-C2, this ratio decreases as the temperature increases. This behavior is qualitatively in agreement with our above analysis. On the other hand, the excitonic emission for N-C1 is still invisible in the time-integrated PL on this scale, because the energy transfer rate is sufficiently high. In fact, the phosphorescence intensity of N-C1 is high enough to observe bright green emissions even at room temperature. We believe that N-C1 will be useful for green light emitting devices.

In order to investigate the temperature dependence of the energy transfer rate, we compare the decay curves of the  $\Gamma_{1,2}^-$  emission for N-C1 and N-C2 at 10 and 300 K. The solid lines and the closed circles in Figs. 5(c) and 5(d) are calculated and observed decay curves, respectively. We can see that the observed curves at 300 K show slower decay than those at 10 K. If the energy transfer is absent, the decay must become faster at higher temperatures because the nonradiative component becomes dominant. In fact, for C4PbBr<sub>4</sub> and N-C6 (i.e., small-energy-transfer system), the observed PL decay times at 300 K were slightly faster than those at 10 K. This strongly indicates that the decay of the  $\Gamma_{1,2}^-$  emission for N-C1 and N-C2 is not determined by the nonradiative decay rate, but by the energy transfer rate even at room temperature. In addition, the observed curves at 300 K show even slower decays than the calculated ones. In the calculation we set  $\tau_{12}$  and  $\tau_{ET}$  constant over temperature. The discrepancy between the experimental and calculated decay curves indicates that the energy transfer rate becomes small at higher temperature. The reason for

this is not clear at the present. This point is quite important for the hybrid system and will be discussed in the near future.

In summary, we observed the efficient energy transfer from Wannier excitons to the triplet state of naphthalene molecules in organic-inorganic hybrid quantum-well materials. Although these materials have a problem in long-time durability so far, this observation opens the possibility of realization of high-performance green light emitting devices, nonlinear optical devices, and particularly hybrid excitons. If we incorporate Frenkel excitons whose singlet energy is equal to that of the Wannier exciton, e.g., anthracene is a good candidate, the highly efficient Dexter mechanism couples the different type excitons forming the hybrid excitons.

- 
- [1] V. Agranovich, R. Atanasov, and F. Bassani, *Solid State Commun.* **92**, 295 (1994).
  - [2] V.M. Agranovich, D.M. Basko, G.C. La Rocca, and F. Bassani, *J. Phys. Condens. Matter* **10**, 9369 (1998).
  - [3] O. Roslyak and J.L. Birman, *Phys. Rev. B* **75**, 245309 (2007).
  - [4] F. Bassani, G.C. La Rocca, and D.M. Basko, *Phys. Solid State* **41**, 701 (1999).
  - [5] J. Ishi, H. Kunugita, K. Ema, T. Ban, and T. Kondo, *Appl. Phys. Lett.* **77**, 3487 (2000).
  - [6] T. Fujita, Y. Sato, T. Kuitani, and T. Ishihara, *Phys. Rev. B* **57**, 12 428 (1998).
  - [7] M. Shimizu and T. Ishihara, *Appl. Phys. Lett.* **80**, 2836 (2002).
  - [8] S. Blumstengel, S. Sadofev, C. Xu, J. Puls, and F. Henneberger, *Phys. Rev. Lett.* **97**, 237401 (2006).
  - [9] G. Itskos, G. Heliotis, P.G. Lagoudakis, J. Lupton, N.P. Barradas, E. Alves, S. Pereira, I.M. Watson, M.D. Dawson, J. Feldmann, R. Murray, and D.D.C. Bradley, *Phys. Rev. B* **76**, 035344 (2007).
  - [10] M. Era, K. Maeda, and T. Tsutsui, *Chem. Phys. Lett.* **296**, 417 (1998).
  - [11] T. Förster, *Ann. Phys.* **2**, 55 (1948).
  - [12] D.L. Dexter, *J. Chem. Phys.* **21**, 836 (1953).
  - [13] P.P. Lima, S.S. Nobre, R.O. Freire, S.A. Junior, R.A. Sa Ferreira, U. Pischel, O.L. Malta, and L.D. Carlos, *J. Phys. Chem. C* **111**, 17 627 (2007).
  - [14] K. Tanaka, T. Takahashi, T. Kondo, K. Umeda, K. Ema, T. Umebayashi, K. Asai, K. Uchida, and N. Miura, *Jpn. J. Appl. Phys.* **44**, 5923 (2005).
  - [15] K. Ema, K. Umeda, M. Toda, C. Yajima, Y. Arai, H. Kunugita, D. Wolverson, and J.J. Davies, *Phys. Rev. B* **73**, 241310(R) (2006).
  - [16] T. Ishihara, J. Takahashi, and T. Goto, *Phys. Rev. B* **42**, 11 099 (1990).
  - [17] K. Tanaka, T. Takahashi, T. Kondo, T. Umebayashi, K. Asai, and K. Ema, *Phys. Rev. B* **71**, 045312 (2005).
  - [18] Y. Kato, D. Ichii, K. Ohashi, H. Kunugita, K. Ema, K. Tanaka, T. Takahashi, and T. Kondo, *Solid State Commun.* **128**, 15 (2003).